*Solar and Stellar Activity: Similarities and Differences*
*ASP Conference Series, Vol. 158, 1999*
*C.J. Butler and J.G. Doyle, eds.*

# Theoretical Chromosphere Models

P. Ulmschneider
*Institut f. Theoret. Astrophysik, Univ. Heidelberg, Tiergartenstr. 15, 69121 Heidelberg, Germany*

**Abstract.** Theoretical chromospheric models depend on four fundamental parameters: effective temperature, gravity, metallicity and rotation period. The physical logic is outlined by which these four parameters determine the observed chromospheres. On the basis of the heating mechanism, mechanical energy fluxes are computed for a wide range of late-type stars and the propagation and dissipation of this energy into the outer stellar layers is evaluated. For stars with a low rotation rate, theoretical chromosphere models based on pure acoustic heating for the Sun and other main sequence stars are discussed.

## 1. Introduction

Despite the fact that the solar chromosphere and corona show large variations in emission across the solar surface as well as during the sunspot cycle, it is well known that the average behaviour of these hot outer stellar layers can only depend on four fundamental parameters, which uniquely define any non-accreting, nondegenerate star. For a single star there are only 3 fundamental parameters, mass, chemical composition and age, while the fourth parameter, rotation, is determined from the angular momentum loss rate and changes in the moment of inertia which are both functions of age. However, because more than 70% of all stars are members of binary or multiple systems, where unknown amounts of orbital angular momentum have been transferred to spin angular momentum, one generally needs to specify the rotation rate independently from the age. Naturally if one considers T-Tauri stars, additional parameters must be specified as e.g. the mass accretion rate. These four fundamental parameters that uniquely specify a star can conveniently be taken to be effective temperature, $T_{eff}$, surface gravity, $g$, metallicity, $Z_m$ and rotation period $P_{Rot}$. The great challenge to the theoretician is to elucidate the physical connection between these four parameters and the observed chromospheres and coronae. It is fortunate that recent advances make it likely that this theoretical aim can be realized in the near future and that reliable theoretical chromosphere models are now in grasping distance.

While in the field of stellar atmospheres the agreement between empirical and theoretical photospheric models based on $T_{eff}$, $g$ and $Z_m$ is usually very good, we are far from a similar reliability of theoretical chromosphere and corona models. There are three properties which particularly distinguish chromospheres and coronae from photospheres: the *magnetic fields*, the stochastic

and secular, spatial and temporal *variability* and the *mechanical heating.* We know that for late-type stars the magnetic fields are not fossil ones, left over from star-formation, but that they are generated by the star itself. The theory which describes how magnetic fields are generated, the dynamo theory, needs two important ingredients: convection and rotation (Choudhuri 1998, Schüssler, Schmidt & Ferriz-Mas 1997, Proctor & Gilbert 1994). Both can be computed or specified on the basis of four fundamental parameters. As a rising convective bubble expands and as horizontal motion on a rotating star leads to Coriolis forces, the generated convective flows are helical. They amplify the magnetic fields and thus create magnetic flux. There is reasonable hope that with massive magnetohydrodynamic simulations the dynamo theory will become highly accurate and predictive in the near future.

The chromospheric and coronal variability derives from the action of the turbulent convection and from magnetic flux emergence. The variability can therefore be explained by modeling the turbulent convection and the time-dependent magnetic flux emergence using the dynamo theory. The same is valid for mechanical heating. It has been known for some time that for the existence of chromospheres and coronae, mechanical heating is absolutely essential. Mechanical energy is produced by wave generation, by foot-point motion of magnetic flux tubes which lead to entangled fields and by magnetic flux emergence. Thus all the peculiar properties of chromospheres should be describable by convection zone models and by the dynamo theory, that is, by theoretical models based on the four fundamental parameters.

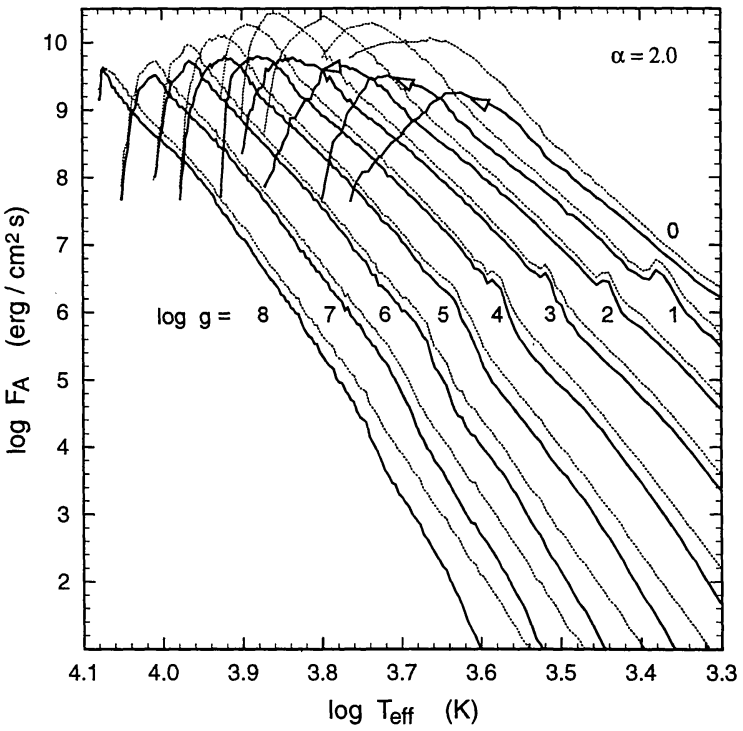


Figure 1. Acoustic fluxes for stars versus $T_{eff}$ for given $\log g$, solar abundance $Z_m = [0]$ and $\alpha = 2.0$.

## 2. Heating Mechanisms

A survey of the proposed heating mechanisms shows that they can be subdivided into two main types, the *hydrodynamic-* and the *magnetic mechanisms* (see e.g. Narain & Ulmschneider 1996). Each of these major types can be further subdivided into fast and slow mechanisms. Fast hydrodynamic mechanisms (where the periods $P$ are less than the acoustic cut-off period $P_A$) are the acoustic waves while the slow mechanisms (usually $P > P_A$) are the pulsational waves. The fast magnetic mechanisms, usually called AC (alternating current) mechanisms, are magneto-acoustic-, Alfvén- and surface waves. Slow magnetic mechanisms, also called DC (direct current) mechanisms, are current sheets and micro-flares. Based on successful terrestrial laboratory experiments a large zoo of different magnetic heating mechanisms has been proposed, particularly of the wave type.

The great difficulty in the nearly sixty years since 1941, when Edlén and Grotrian first recognized the solar corona as an extremely hot outer layer, was and is, to identify which heating mechanism is important in the stellar environment and in a given magnetic field configuration on the star. The problem is that it became clear that the heating by mechanical energy typically occurs in regions of very small scales, say in the meter-range on the Sun. This refers to the shock structure region in a shock wave and the current carrying region in a current sheet. Unfortunately, despite of the great recent technological advances to improve the resolution of solar observations it is presently still hopeless to resolve scales in the meter-range. Because of the lacking resolution on the Sun, for instance, it cannot easily be decided whether a non-magnetic region is heated by acoustic shock waves, or by some magnetic mechanism which operates in a weak or unresolved field. Here stellar observations come to the rescue.

It seems utterly surprising that from stellar observations, where entire stars are reduced to point sources, information can be obtained about heating properties in the meter-range. The reason why stellar observations are so crucial in unraveling the important heating mechanisms is that by selecting different stars, the observer can vary $T_{eff}$ by one, $g$ by five, $Z_m$ by three and $P_{Rot}$ by two orders of magnitude. In addition, stellar observations naturally integrate over the surface of the star and thus make easier a comparison with a theory which predicts the average behaviour (plus its range of variability). By computing mechanical energy generation rates and by producing theoretical chromosphere models for different stars it is possible to compare the simulated chromospheric emission fluxes with the observed ones. Any heating mechanism which survives such a rugged comparison over many orders of magnitude in variation of the entire set of fundamental stellar parameters must without doubt be considered identified. This procedure allowed us to finally identify acoustic waves as the basic chromospheric heating mechanism for slowly rotating (large $P_{Rot}$) non-magnetic stars. Presently the same identification method is also applied to magnetic mechanisms (see the contribution of M. Cuntz, this volume) to unravel the heating mechanism of magnetic chromospheres.

### 2.1. Acoustic Wave Energy Generation

The theory of sound generation from turbulence was developed in the early 1950's by Lighthill and Proudman and was further extended by Stein to stellar

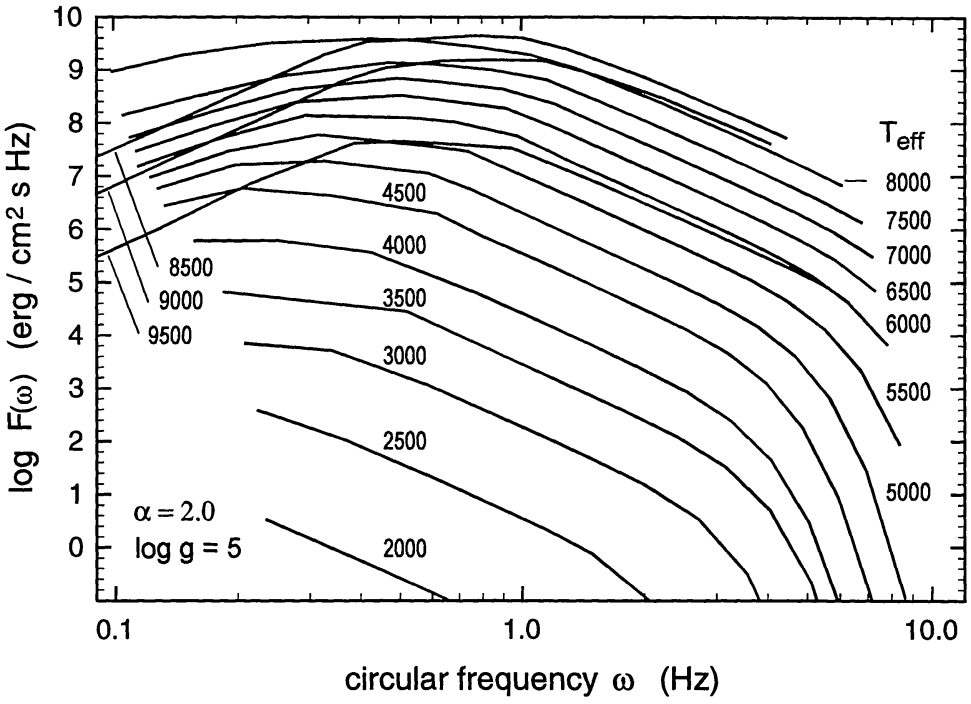


Figure 2. Acoustic spectra for stars versus circular frequency for given $T_{eff}$, $Z_m = [0]$ and $\alpha = 2.0$, with $\log g = 5$.

convection zones. The Lighthill-Stein theory has been re-discussed in detail by Musielak et al. (1994), who found that the stellar turbulence is best represented by a Kolmogorov-type energy spectrum. By specifying $T_{eff}$, $g$, $Z_m$ and the mixing-length parameter $\alpha$, convection zone models were computed and the emergent acoustic flux as well as the acoustic frequency spectrum evaluated on basis of the Lighthill-Stein theory. For $\alpha$, the ratio of the mixing-length to the scale height, one typically has $\alpha \approx 1.5$ to 2.0. Figures 1 and 2 show acoustic fluxes as well as acoustic energy spectra computed this way for a large number of late-type stars in the HR-diagram (after Ulmschneider, Theurer & Musielak 1996). While in terrestrial situations, monopole, dipole and quadrupole sound generation is a sequence of progressively less important ways to produce acoustic waves, quadrupole sound generation is the dominant contribution in stellar situations.

As the acoustic energy generation depends mainly on the convective velocity and because convection zone models do not depend on stellar rotation it is clear that the acoustic energy flux does not depend on rotation. However, there is a strong dependence on metallicity. Figure 3 shows the dependence of the acoustic flux on $Z_m$ for main sequence stars (with $\log g = 4.44$) after Ulmschneider et al. (1998). $Z_m = [0]$ means solar metallicity, $Z_m = [-1]$, 1/10 solar metal content etc. It is seen that for stars with $T_{eff} > 5000\ K$, where hydrogen is the main opacity, the acoustic flux does not depend much on $Z_m$, but that for cooler stars, where the opacity is dominated by metals, the acoustic flux decreases by an order of magnitude for every reduction of the metal content by a factor of ten. This

is explained by the fact that a reduction of the surface opacity leads to a shift of the top of the convection zone, the level where the optical depth is roughly unity, to deeper layers where the density is larger and the convective velocities correspondingly smaller. Figures 1 & 3 show that there is a nine orders of magnitude variation of the acoustic flux with the fundamental parameters $T_{eff}$, $g$ and $Z_m$, but no variation with $P_{Rot}$.

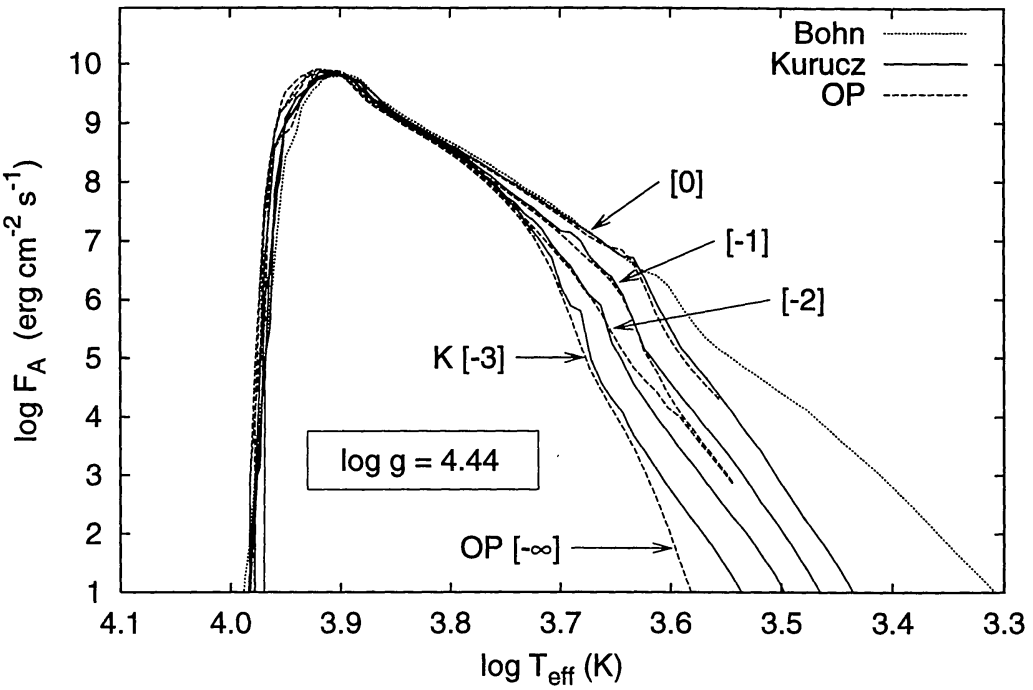


Figure 3. Acoustic fluxes for main sequence stars of $\log g = 4.44$ versus $T_{eff}$ for different metallicity $Z_m$ (indicated in brackets) and $\alpha = 2.0$.

## 2.2. Magnetic Wave Energy Generation

The magnetic field at the solar photosphere outside of sunspots and pores appears in the shape of flux tubes which are concentrated in the convection zone by the granular and super-granular flows and the convective collapse. The turbulent motions in the non-magnetic convection zone outside strangles and displaces the magnetic flux tubes, which leads to the generation of longitudinal and transverse MHD waves, respectively. Simulating the turbulent motions on the basis of convection zone models, pressure and velocity fluctuations can be applied to the flux tubes and the generated longitudinal MHD tube wave and transverse Alfvén wave fluxes can be computed. Such computations after Huang, Musielak & Ulmschneider (1995) and Ulmschneider & Musielak (1998) are shown in Figure 4. Due to the stochastic nature of the turbulence occasionally large velocity spikes occur which approach 3 km/s, in good agreement with observations. This leads to a very stochastic behaviour of the generated instantaneous wave flux seen in Figure 4.

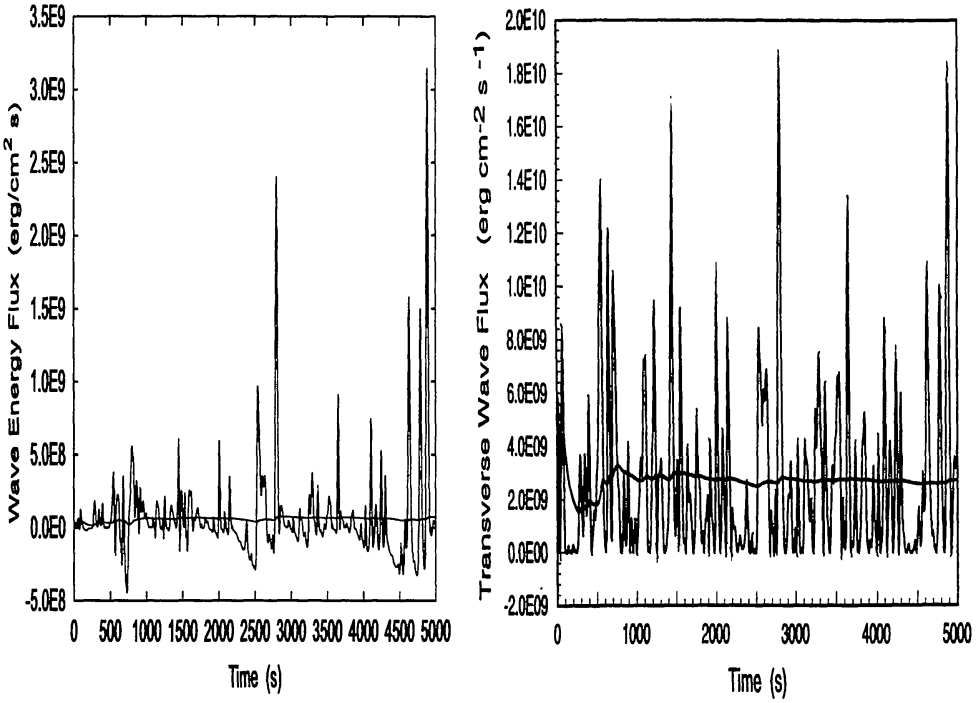


Figure 4. Instant and time-averaged longitudinal and transverse tube wave energy fluxes versus time.

Applying these calculations to stars other than the Sun the magnetic field strength $B_0$ of the flux tubes at the stellar surface must be known. Here in analogy to the Sun various fractions of the equipartition field strength $B_{eq} = \sqrt{8\pi p_0}$ have been assumed, where $p_0$ is the gas pressure at the stellar surface. In the future, time-dependent simulations of the convective collapse will provide a definite ratio $B_0/B_{eq}$. Figure 5 shows longitudinal tube wave fluxes for late-type stars in the HR-diagram computed by Ulmschneider, Musielak & Fawzy (1998). It is seen that these fluxes have a distinctively different behaviour on $T_{eff}$ and $g$ compared to the acoustic fluxes.

## 3. Wave Propagation

From Figure 2 it is clear that a computation of the acoustic wave propagation must start from the acoustic flux and the acoustic frequency spectrum generated in the stellar convection zone. Calculations using acoustic spectra have been undertaken by e.g. Carlsson & Stein (1994, 1995) and Theuer, Ulmschneider & Kalkofen (1997). In monochromatic wave computations (Buchholz, Ulmschneider & Cuntz 1998), the atmosphere becomes permeated by a series of sawtooth shaped shock waves of constant (limiting) strength which depends on the wave period $P$. A calculation using an acoustic wave spectrum shows a quite different behaviour as shown in Figure 6 from Theurer (1998). Here the merging of numerous small shocks generates typically a single large, long-period shock, plus a few smaller shocks similar to those in a monochromatic calculation.

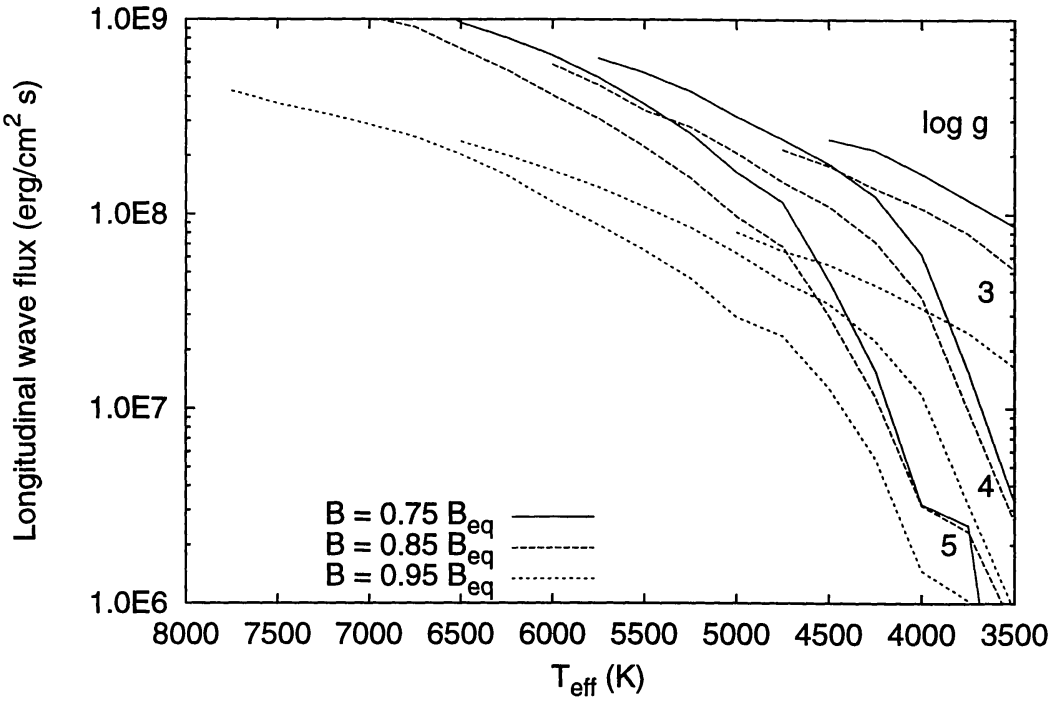


Figure 5. Longitudinal tube wave fluxes for stars versus $T_{eff}$ for given $\log g$, with solar metallicity $Z_m = [0]$, $\alpha = 2$ and different ratios of magnetic field strength $B_0/B_{eq}$.

Aside of the fact that all computations so far are plane wave calculations which neglect important acoustic refraction and standing wave effects, these most recent calculations still suffer from some unfortunate approximations. The calculations of Theuer et al. (1997) neglect the fully time-dependent ionization of hydrogen, as well as its ionization energy in the energy equation. Both effects lead to the fact that the single large shock in Figure 6 is much too strong and consequently the simulated chromospheric emission is too large. Yet the smaller shocks lower in the atmosphere are adequately described. Stein & Carlsson (1994, 1995), who use a code which includes the fully time-dependent hydrogen ionization and the hydrogen ionization energy, obtained results which suffer from an unfortunate choice of the acoustic input spectrum. Figure 7 (from Theurer et al. 1997) shows two acoustic spectra at height $z = 250\ km$ in the Sun computed on basis of a full Kolmogorov-type acoustic spectrum generated in the convection zone at height $z = -160\ km$. The spectrum on the right hand side would be seen in terrestrial observations because it includes the effect of the modulation transfer function, while the left hand spectrum is actually supposed to be present at $z = 250\ km$ height. The modulation transfer function tells what fraction of a given velocity oscillation can be seen as Doppler shift fluctuation in a spectral line. A low lying Fe-line is formed over a height interval of about 300 km, which for a sound speed of 7 km/s corresponds to the wavelength of a wave with a period of about $P = 40\ s$. For periods $P < 40\ s$, the velocity fluctuations no longer show themselves as Doppler shifts but as line-broadening, which results in

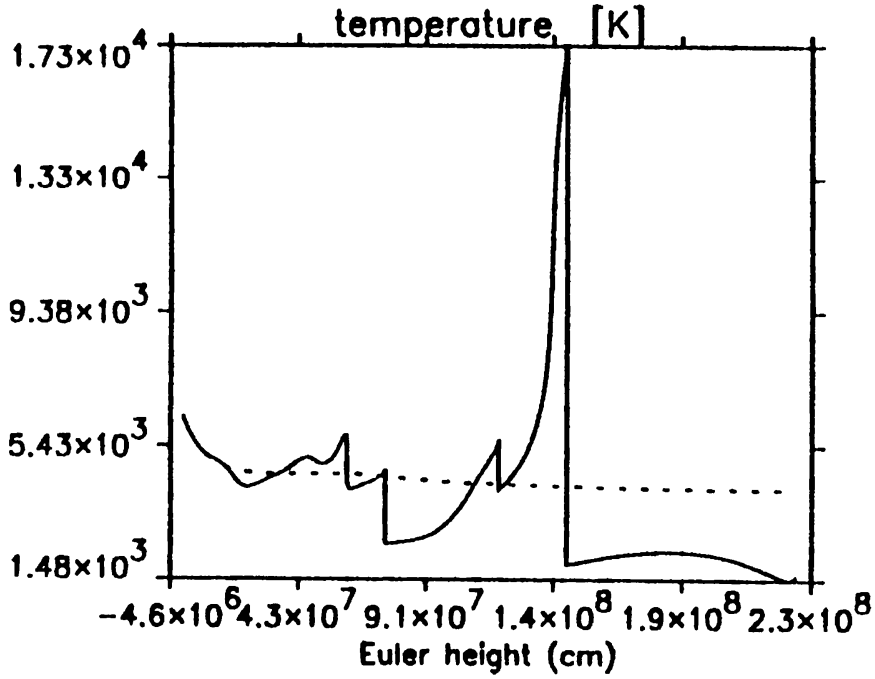


Figure 6. Instantaneous temperature as function of height in the solar atmosphere for an acoustic wave calculation starting from an acoustic spectrum in the convection zone, at time 3680 s. The dotted line is the initial radiative equilibrium temperature distribution.

the decrease of the modulation transfer function to zero. Observing solar velocity fluctuations in a low-lying Fe-line one thus detects only a small part (the long-period part) of the entire acoustic spectrum. Because of this effect the Carlson & Stein calculations, using such observed fluctuations as input, found only the single large long-period shock and no smaller shocks. Although it is clear that these temporary defects will shortly be overcome and wave calculations using the appropriate acoustic spectra will shortly be available, it must be pointed out that monochromatic calculations with adequately chosen wave period, by avoiding the above pitfalls, can provide reasonably reliable results.

## 4. Line Emission, Comparison of Theory and Observation

After running a radiation-hydrodynamic wave code for a sufficiently long time, the atmosphere reaches a dynamical steady state in which the averaged quantities become time-independent. A powerful diagnostic tool is then to simulate the chromospheric Ca II H&K and Mg II h&k lines and compare their emission flux with observations. Figure 8 (after Theurer 1998) shows the emerging Ca II K line profiles using partial redistribution (PRD) for solar wave calculations using an acoustic spectrum (labeled bKmG) and two monochromatic wave cases with $P = 20$ and 40 $s$ (labeled mP20, mP40), all with the same acoustic energy flux. Due to the single very strong shock both the total emission and

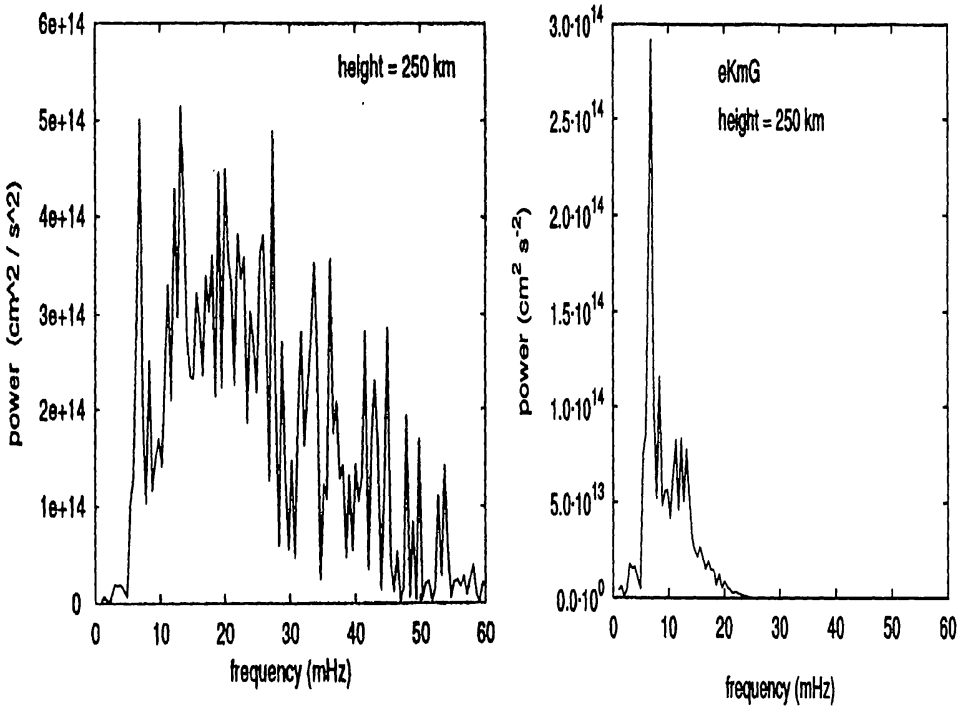


Figure 7. Theoretical acoustic spectra in the solar atmosphere at height $z = 250$ $km$. The left panel shows the actual spectrum, while the right panel the 'observed' spectrum with the modulation transfer function applied.

the line-asymmetry are exaggerated in the acoustic spectrum case. Aside of this effect, however, the two time-averaged bKmG and mP40 line-profiles appear to be fairly similar, which shows that a monochromatic wave calculation, with the right choice of the wave period (near the maximum of the acoustic spectrum), can give reasonable results.

Figure 9 shows a comparison of the theoretical and observed chromospheric emission fluxes in the Ca II and the Mg II lines of late-type stars versus the color index B-V after Buchholz et al. (1998). Observations indicate that main-sequence (dots) and giant stars (triangles) occupy the same empirical minimum emission line (solid) in the diagram, called *basal flux line*, which is interpreted as the result of pure acoustically heated chromospheres. Dots and triangles above this line represent stars which have additional magnetic heating, correlated with rotation. The theoretical simulations (x's for main-sequence and circles for giant stars) are obtained from the generated acoustic wave fluxes using monochromatic waves. It is seen that the basal flux line is well reproduced. A similar calculation of theoretical Ca II and Mg II line emissions of giants with metallicities $Z_m = [-1]$ and $Z_m = [-2]$ (Cuntz, Rammacher & Ulmschneider 1994) shows that these stars also fall on the basal flux line in agreement with observations. This nice agreement over a wide range of fundamental parameters $T_{eff}$, $g$ and $Z_m$ shows that acoustic waves can now be considered as a firmly established heating mechanism for chromospheres of stars with large rotation period $P_{Rot}$.

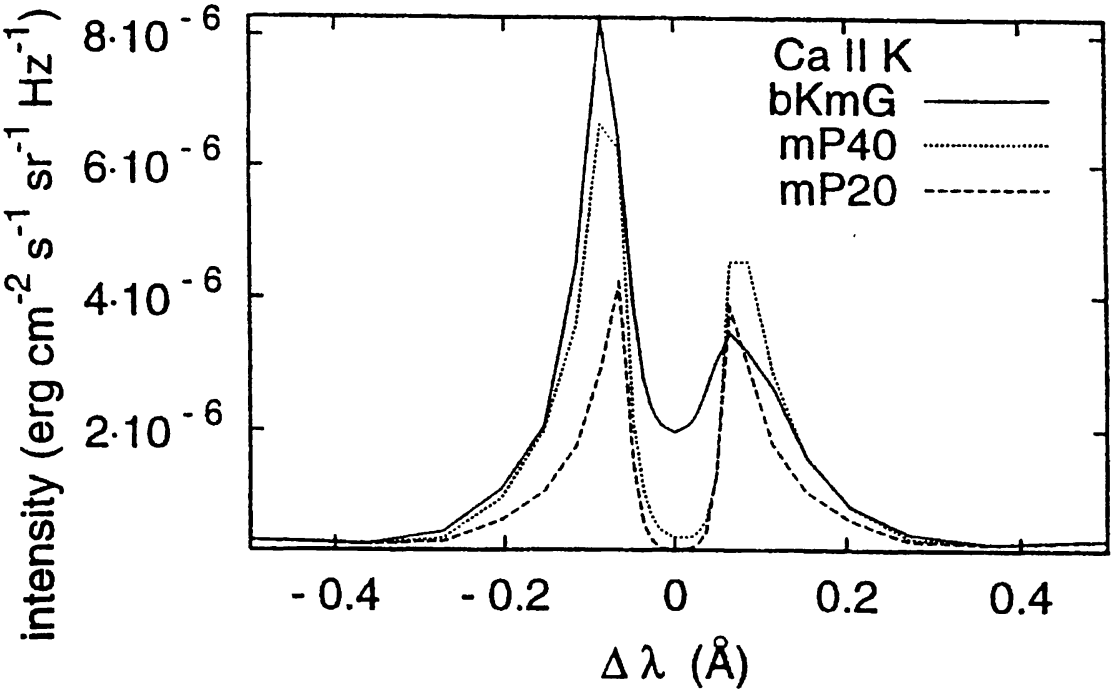


Figure 8. Theoretical time-averaged Ca II K-line profile with partial redistribution (PRD) for calculations using two monochromatic wave cases (P=20, 40 s) and a case with an acoustic spectrum (bKmG).

## 5. Theoretical Chromospheres

Let us now address the topic of theoretical chromosphere models. Figure 10 (from Theurer 1998) shows theoretical time-averaged temperature profiles for the chromosphere of the Sun. The line marked $T_0$ shows the radiative equilibrium atmosphere before the start of the wave calculation. The lines marked mP20, mP40 and bKmG indicate the averaged temperatures of two monochromatic wave cases (with period $P = 20,\ 40\ s$) and a calculation with an acoustic Kolmogorov-type spectrum, all with the same initial acoustic energy. It is seen that the acoustic spectra case shows a large temperature depression below the $T_0$ distribution. This is a well known effect (Ulmschneider et al. 1978), caused by the very strong shock and the nonlinearity of the Planck function and must be considered as an artifact. It is significant that all three wave models above 1400 km height show an outward temperature rise as is present in a classical chromosphere. We are convinced that a better treatment of the single strong shock will bring the acoustic spectrum (bKmG) result much closer to the mP40 case. Comparing Figure 10 to Figure 5 of Carlsson & Stein (1994, also 1995) it is seen that their time-averaged temperature, which decreases in an outward direction almost completely coincides with our radiative equilibrium temperature distribution $T_0$. These authors conclude that a non-magnetic chromosphere is essentially an outwardly decreasing radiative equilibrium layer on top of which single strong shocks propagate. The emission from such shocks then was wrongly

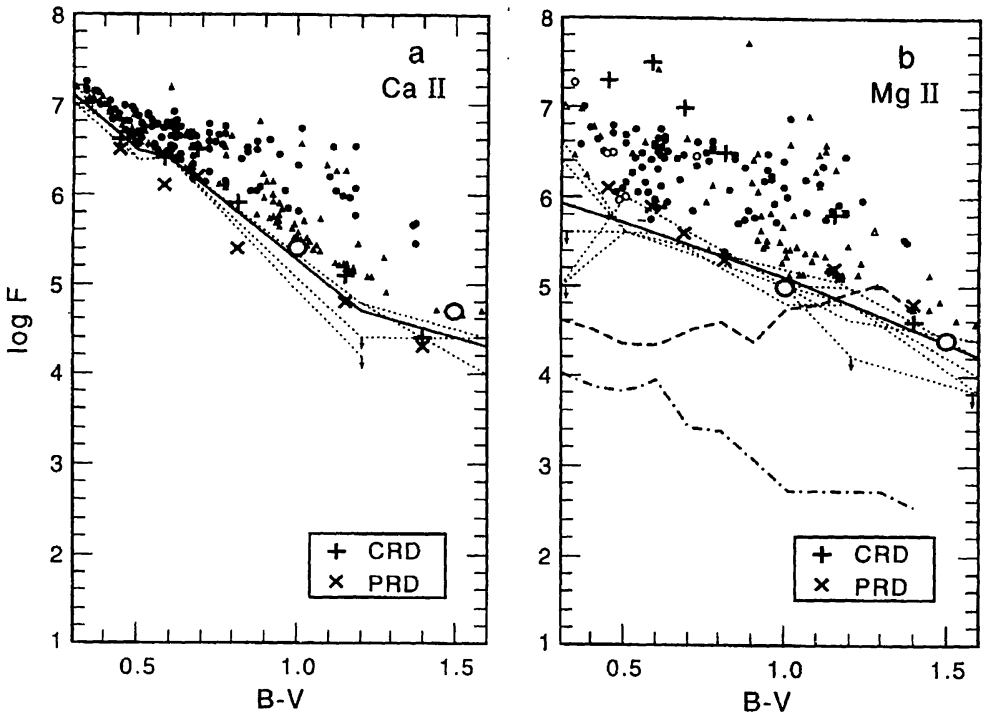


Figure 9. Theoretical and empirical chromospheric emission fluxes in the Ca II and Mg II lines versus colour for late-type stars.

attributed by empirical models to a classical chromosphere with an outwardly rising mean temperature distribution. We believe that some of the conclusions of Carlsson & Stein are a direct consequence of the neglect of the largest fraction of the acoustic spectrum. A treatment of the full spectrum would also produce the little shocks and thus would lead to a remnant of the classical chromosphere, that is, to an outwardly rising mean temperature. Clearly, however, both Carlsson & Stein's and our calculations indicate, that single large shocks are a persistent feature in the chromosphere and that the emission from shock waves is a dominant effect which must be taken into account when constructing empirical models.

Figure 11 (from Buchholz et al. 1998) shows the mean temperature distribution of six theoretical chromosphere models for main sequence stars ranging from spectral type F5V to M0V. Also shown are the corresponding initial radiative equilibrium distributions. Due to the low acoustic energy fluxes of M-stars, their photospheres extend to very low mass column density $m$, where finally shock formation leads to heating and a chromospheric temperature rise develops. For earlier spectral type the acoustic fluxes are much larger and the location of the temperature minimum and the associated chromospheric temperature rise shifts to greater mass column density. For the earliest spectral types a large temperature depression below the radiative equilibrium values develops. This is the result of large amplitude acoustic waves. These calculated properties of theoretical chromosphere models are in nice qualitative agreement with empirical models by Kelch, Linsky & Worden (1979) based on Ca II line observations.

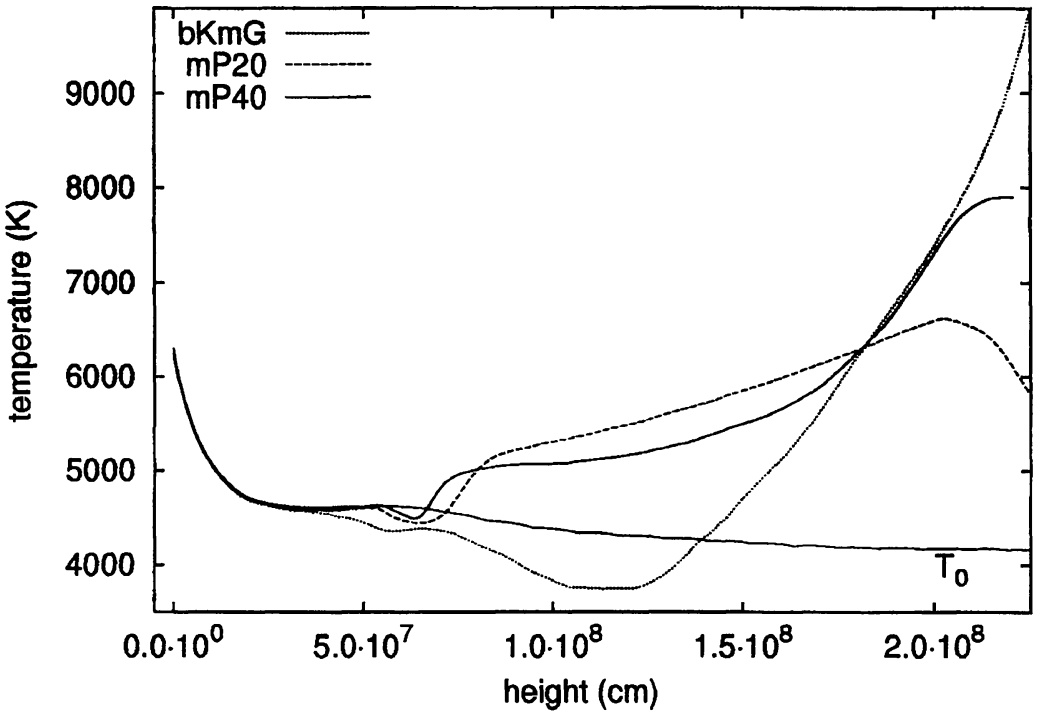


Figure 10. Time averaged solar temperature distributions for two monochromatic wave calculations (mP20, mP40) and a one using an acoustic spectrum (bKmG). Also shown is the initial radiative equilibrium distribution ($T_0$) before the start of the wave computations.

The large temperature depression in the theoretical models is connected to the large 'photospheric temperature excess' in the Ca II line models. One urgently looks forward to more reliable chromosphere models in the future, based on the full acoustic spectra. Ultimately acoustic chromosphere models as function of $T_{eff}$, $g$ and $Z_m$ should become as reliable as the present photosphere models for slowly rotating stars. With the identification of the magnetic heating mechanisms, where $P_{Rot}$ comes into play, this may even be true for the chromosphere models of all late-type stars which depend on the full set of four fundamental parameters.

**Acknowledgments.** I want to thank my collaborators B. Buchholz, M. Cuntz, D. Fawzy, Z.E. Musielak, W. Rammacher and J. Theurer who all contributed to this work, and NATO for grant CGR-910058.

## References

Buchholz B., Ulmschneider P. & Cuntz M., 1998, ApJ, 494, 700

Carlsson M. & Stein R.F., 1994, *'Chromospheric Dynamics', mini-workshop*, Univ. of Oslo, M. Carlsson Ed., p. 47

Carlsson M. & Stein R.F., 1995, ApJ, 440, L29

Choudhuri A.R., 1998, The Physics of Fluids and Plasmas, Camb. Univ. Press

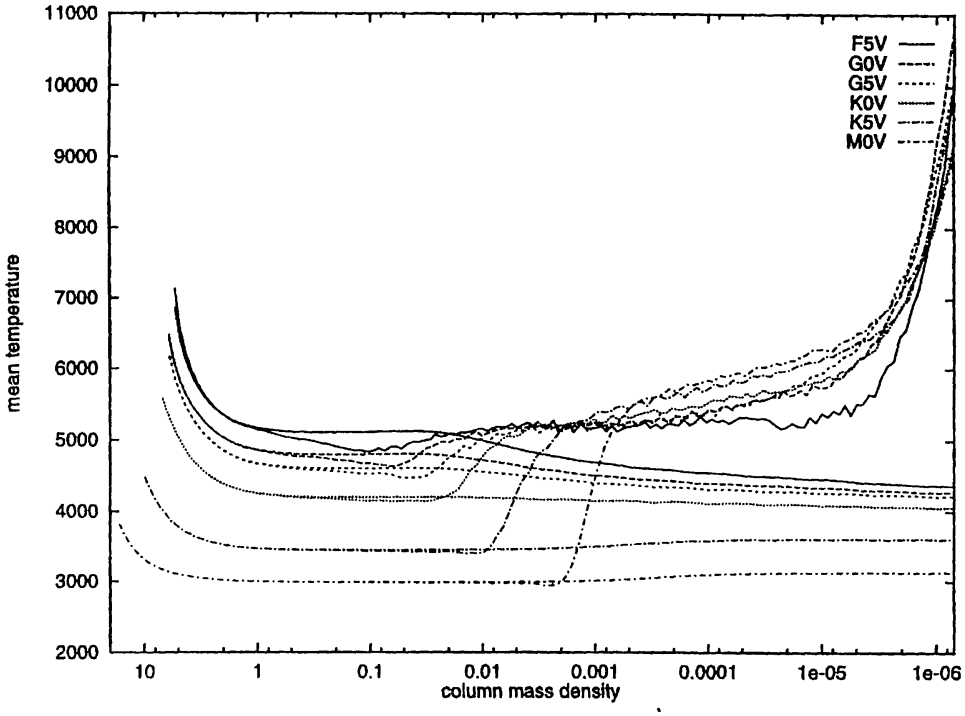


Figure 11. Time-averaged temperature distributions for six main-sequence stars based on monochromatic calculations. Also shown are the corresponding initial radiative equilibrium distributions.

Cuntz M., Rammacher W. & Ulmschneider P., 1994, ApJ, 432, 690

Huang P., Musielak Z.E. & Ulmschneider P., 1995, A&A, 297, 579

Kelch W.L., Linsky J.L. & Worden S.P., 1979, ApJ, 229, 700

Musielak Z.E., Rosner R., Stein R.F. & Ulmschneider P., 1994, ApJ, 423, 474

Narain U. & Ulmschneider P., 1996, Space Sci.Rev., 75, 453

Proctor M.R.E. & Gilbert A.D., 1994, Lectures on Solar and Planetary Dynamos, Cambridge Univ. Press

Schüssler M., Schmitt D. & Ferriz-Mas A.: 1997, in: Advances in Physics of Sunspots, ASP Conf. Ser. 118, B. Schmieder, J.C. del Toro Iniesta & M. Vazquez Eds., p. 39

Theurer J.: 1998, Ph.D. thesis, Univ. Heidelberg

Theurer J., Ulmschneider P., Kalkofen W., 1997, A&A, 324, 717

Ulmschneider P. & Musielak Z.E., 1998, A&A, 338, 311

Ulmschneider P., Musielak Z.E. & Fawzy D.:, 1999, A&A, to be submitted

Ulmschneider P., Schmitz F., Kalkofen W. & Bohn H.U.: 1978, A&A, 70, 487

Ulmschneider P., Theurer J. & Musielak Z.E., 1996, A&A, 315, 212

Ulmschneider P., Theurer J., Musielak Z.E. & Kurucz R., 1998, A&A, to be submitted